Double Fano resonances in disk-nonconcentric ring plasmonic nanostructures*

ZHANG Xingfang[1,2], LIU Fengshou[1], LIANG Lanju[1,2], and YAN Xin[1]**

1. School of Opt-Electronic Engineering, Zaozhuang University, Zaozhuang 277160, China

2. Laboratory of Optoelectronic Information Processing and Display of Shandong, Zaozhuang 277160, China

(Received 9 April 2023; Revised 14 July 2023)

The plasmonic properties of gold nanostructures composed of a disk outside a nonconcentric ring are numerically studied by the finite difference time domain (FDTD) method. Simulated results show that two Fano resonances are formed as a result of the coupling of the octupolar and quadrupolar modes of the ring with the dipolar mode of the disk. The reduction in structural symmetry causes a red shift of the Fano resonances and distinct changes in spectral lineshape by offsetting the center of the inner surface of the ring to different directions. The effects of several geometric parameters on the characteristics of Fano resonances are also discussed. In addition, the refractive index (*RI*) sensitivities for the two Fano resonances can be up to 581 nm/RIU and 780 nm/RIU with the corresponding figure of merits (*FOMs*) as large as 12.7 and 10.2, respectively. Such properties render the structures useful for potential applications in multi-wavelength sensors.

Document code: A **Article ID:** 1673-1905(2024)01-0001-6

DOI https://doi.org/10.1007/s11801-024-3064-y

Fano resonance caused by the destructive interference of a broad superradiant bright mode with a narrow subradiant dark mode in plasmonic nanostructures has gained much attention in the past few decades[1]. One of the characteristics of Fano resonance is the obvious sharp and asymmetric lineshape in the broad scattering or extinction spectrum[2,3], which is highly sensitive to the subtle changes in the surrounding medium, thereby it is helpful to design various high-sensitivity sensors, such as biochemical sensors[4] and refractive index sensors[5]. The extremely huge local field enhancement generated in the vicinity of the nanostructure, due to the energy exchange between the bright mode and the dark mode by near field coupling, is another striking optical feature of Fano resonance[6], and accordingly many light-matter interactions requiring strong field can be carried out, such as second harmonic generation[7], spasers[8], etc. Up to now, various Fano nanostructures have been proposed and investigated in both numerical simulations and experiments, and it is found that the spectral position and lineshape of Fano resonance are closely related to structural geometric parameters[9], chemical composition[10], and spatial arrangement[11].

To break through the limitations of optical devices based on single Fano resonance in certain applications, the excitation of multiple Fano resonances has recently attracted considerable interest for great potential in surface-enhanced Raman spectroscopies[12], multiband sensors[13], and so on, since it can simultaneously control the interaction between light and matter at several wavelengths. There are two common ways to obtain multiple Fano resonances. One is to use oligomers or clusters composed of several particles, and multiple Fano resonances come from the interaction between multiple dark and bright modes supported by out-of-phase and in-phase particles, respectively[14]. The other is to excite the inherent multipolar dark modes of large-sized particles in simple plasmonic systems. A nanoring is commonly used as a structural element to produce multiple Fano resonances because it supports multipolar dark modes[15]. When a particle is inserted into the nanoring, the conditions for the formation of multiple Fano resonances are likely to be satisfied through a careful structural design[16], and can be found as a result of the interaction between the bright electric and the dark magnetic modes[17]. On the other hand, the nanostructures with the disk outside the nanoring can also produce multiple Fano resonances[18,19]. When there are disks inside and outside the nanoring, more complex multiple Fano resonances can be realized, because multipolar dark modes of the concentric ring-disk nanostructures are excited[20].

According to the plasmon hybridization theory, symmetry breaking in the nanoring via introducing a split gap[21] or making the nanoring thickness uneven[22] can

* This work has been supported by the Qingchuang Science and Technology Plan of Shandong Universities (No.2019KJN001), and the Project Special Funding of Taishan Scholar, China (No.201909150).

** E-mail: zxf4114@126.com

bring fantastic plasmonic features due to a dramatical change in the coupling of the primitive modes, giving rise to a striking modulation of Fano resonance[23]. Further symmetry breaking in the nanostructures can induce more higher-order Fano resonances related to the symmetric and antisymmetric multipolar modes of nanorings[24]. Although Fano resonances in disk-ring nanostructures have been extensively discussed, most investigations focus on the plasmonic properties of particles within the nanoring. There are few reports on the evolution of multiple Fano resonances in nanostructures composed of a particle outside a nonconcentric nanoring (NCNR). In this paper, such nanostructures are investigated numerically using the finite difference time domain (FDTD) method, and the scattering spectra and electric field distributions are simulated to help understand the underlying mechanisms of the formation of multiple Fano resonances. Influences of geometric parameters on the modulation of these Fano resonances are also discussed. The potential of such structures as a biosensor is also evaluated by the refractive index (*RI*) sensitivity and figure of merit (*FOM*). Such characteristics may make the nanostructures suitable for spectral line shaping and biochemical sensing.

Fig.1 illustrates the schematic of our proposed disk-NCNR nanostructure composed of a disk with radius R outside an NCNR with outer and inner radii of R_1 and R_2, respectively. The gap between the disk and the NCNR is D. The offset Δ_x and Δ_y respectively denote a center displacement of the NCNR inner surface in relation to the outer surface along the x and y axis. If Δ_x or Δ_y<0, it means the inner surface moves in a negative direction, conversely, Δ_x or Δ_y>0.

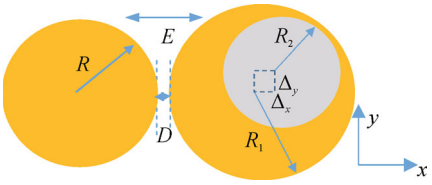

Fig.1 Schematic of the disk-NCNR nanostructure

The nanostructure is normally illuminated by a plane wave propagating in the −z direction with x polarization, and the plasmonic properties are simulated by the three-dimensional FDTD method[25], where the simulation domain is truncated by the perfectly matched layers of absorbing boundaries in all directions and discretized by a grid mesh with the grid step of 2.5 nm in x, y, and z directions. Gold is chosen as the material and its dielectric constants are obtained from the bulk value measured by Johnson and Christy[26]. Unless otherwise specified, the background *RI* is assumed to be n=1, and the height of the structure is set to be H=30 nm, other geometric parameters are R=150 nm, R_1=150 nm, R_2=120 nm, and D=10 nm, respectively. Before simulating the optical properties of our proposed structure, we have confirmed the reliability of our simulation by testing the results of multiple publications.

The plasmonic properties of the disk-NCNR structure in the absence of the offset (Δ_x=Δ_y=0) are firstly considered, the simulated scattering spectrum is shown by the black curve in Fig.2. For comparison, the scattering spectra of a single disk and a single NCNR with the same physical parameters are also given in Fig.2, respectively represented by the blue and red curves. Obviously, the isolated disk and NCNR exhibit typical dipole modes with resonance wavelengths around 876 nm and 1 376 nm, respectively, while the disk-NCNR structure displays the emergence of two Fano dips at the wavelengths of 851 nm and 682 nm as well as a strong peak located at the wavelength of 1 567 nm. The latter is assigned to the bonding dipole mode based on the plasmon hybridization theory. The underlying mechanisms of the formation of these two Fano resonances can be revealed by the distributions of the electric field component E_z at the marked wavelengths, as shown in the insets in Fig.2. Note that for better illustration, the color scales on each inset (not shown) are different, including other insets associated with the E_z distribution below. One can clearly distinguish that the two Fano resonances separately arise from the coupling of the quadrupolar and octupolar modes of the NCNR with the dipolar mode of the disk, since four well-distributed field antinodes appear along the NCNR surface shown in the upper inset, and six antinodes exist in the lower inset.

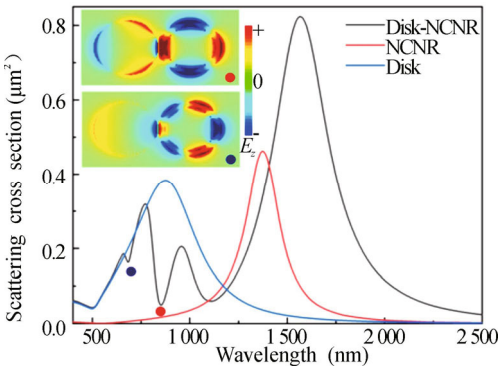

Fig.2 Scattering spectra of the disk, NCNR and disk-NCNR in the absence of offset (Insets show the distributions of near-field component E_z at the marked spectral positions)

Symmetry breaking in the nanoring induced by the thickness nonuniformity renders the higher-order multipolar dark modes dipole active[22], resulting in changes in plasmonic characteristics of disk-NCNR. Fig.3 shows the scattering spectra of the disk-NCNR with different values of offset Δ_x from −20 nm to 20 nm. As is expected, there are obvious changes in the spectral position and contrast ratio of the two Fano resonances. Both Fano dips are red-shifted as the absolute value of Δ_x increases, the reason is that symmetry breaking in the nanoring not only excites the multipolar dark modes but also causes them to undergo a red shift, thereby the coupling of the

red-shifted nanoring resonances with the disk dipole results in the Fano resonances moving towards lower energies. Interestingly, unlike the case as Δ_x increases, the spectral contrast ratio of the two Fano resonances becomes worse as Δ_x decreases from 0, which is similar to the spectral changes obtained in Ref.[27]. When Δ_x decreases to −20 nm, the quadrupole-based Fano dip gets tiny and the octupolar one turns to be a kink. In view of the variation of Fano dips, it can be inferred that as the center of the NCNR inner surface approaches the disk, the coupling between the dipole of the disk and the multipole of the NCNR gets weaker. This is also verified by comparing the near field $|\boldsymbol{E}|$ distribution of the octupole-based Fano resonance at Δ_x=−20 nm with that at Δ_x=20 nm, as shown in the upper two insets in Fig.3. Here, the near field $|\boldsymbol{E}|$ distributions are plotted on the middle plane cutting in the structure and normalized by the incident wave. They have the same color scale. One can find that the near field $|\boldsymbol{E}|$ in some special regions of the NCNR with Δ_x=20 nm is much stronger than that with Δ_x=−20 nm, meaning that the incident energy from the disk is more effectively transferred to the NCNR in the former case. In addition, for the octupolar mode, more field antinodes are located on the thinner shell of the NCNR, as can be seen from the E_z distributions shown in the lower two insets. When Δ_x=20 nm, the left three field antinodes of the NCNR have a positive action with the dipole mode of the disk. As for Δ_x=−20 nm, only the leftmost field antinode of the NCNR has a positive action with the dipole mode, while the other two have a negative action. Maybe this is the reason that the Fano resonances become weaker as the center of the inner surface of the nanoring gets closer to the disk.

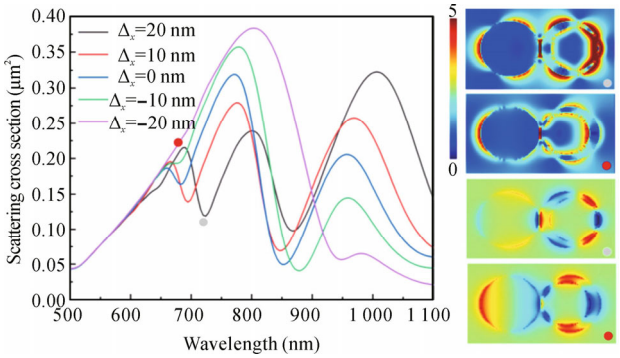

Fig.3 Scattering spectral evolution of the disk-NCNR versus the offset Δ_x (Insets show corresponding E_z (lower two) and electric field intensity $|\boldsymbol{E}|$ distributions (upper two) at the marked wavelengths)

Fig.4 shows the scattering spectra of the disk-NCNR structure as a function of the offset Δ_y. It is found that with an increase of Δ_y, the two Fano dips exhibit a distinct red shift. At the same time, the spectral contrast ratio is increased for the octupole-based Fano resonance, while for the quadrupolar one, it changes little though the scattering intensity is increased at the dip wavelength. For the NCNR in our case, the scattering spectra dependence on the polarization is found to be relatively weak, since the spectral position and scattering intensity of the quadrupolar mode observed for Δ_y=20 nm are almost the same as those for Δ_x=20 nm (data not shown). Consequently, the Fano dips undergo a red shift as the nonuniformity of the nanoring thickness increases. As for the increased spectral contrast ratio of the octupole-based Fano resonance with an increase of Δ_y, this can be understandable because when the octupolar mode gradually approaches the dipolar one, a stronger near field between them could transfer more incident energy from bright mode to dark mode and therefore gives rise to an increasing dip. Concomitantly, the change in the scattering spectrum near the quadrupole-based Fano resonance is caused by the quadrupole of the NCNR getting far away from the disk dipole as Δ_y increases. The phenomenon is analogous to the transmittance evolution observed in the nanoring dimer as the size of the large nanoring increases[28], where the resonance frequencies of the dark quadrupole of the large nanoring and the bright dipole of the nearby small one could coincide with each other first and then turn to be detuned as the former size increases.

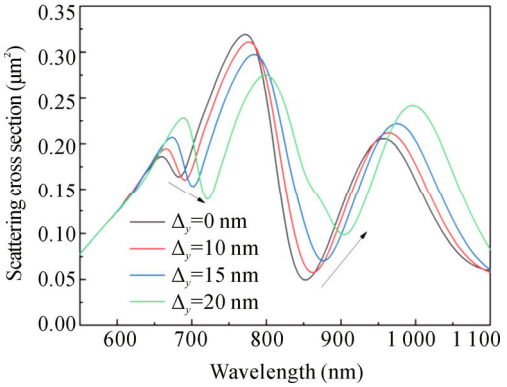

Fig.4 Scattering spectral evolution of the disk-NCNR versus the offset Δ_y

In order to get the dependence of Fano resonances on geometric parameters of the structure, the scattering spectra of the disk-NCNR as a function of R, R_1, R_2, and D are respectively shown in Fig.5. Here, the disk-NCNR with offset Δ_x is chosen. In each simulation, the narrowest region of shell thickness in NCNR $\Delta W=R_2-R_1-\Delta_x$ and the height H are fixed at 10 nm and 30 nm, respectively, while other parameters are kept and their values are the same as those used in Fig.2 except the parameter to be studied.

As shown in Fig.5(a)—(c), one can observe that the two Fano dips are red-shifted monotonously with a decrease of D or an increase of R or R_2. As described in Fig.2, the formation of the Fano resonances is attributed to the coupling of the dipolar mode of the disk with the higher-order multipolar modes of the NCNR. Along with an increase in the gap D, the coupling strength between the bright and dark modes is decreased. Hence, less energy is transferred from the dipole to the multipolar modes, resulting in weakening Fano resonances. Especially, when D increases to 40 nm, the octupolar Fano

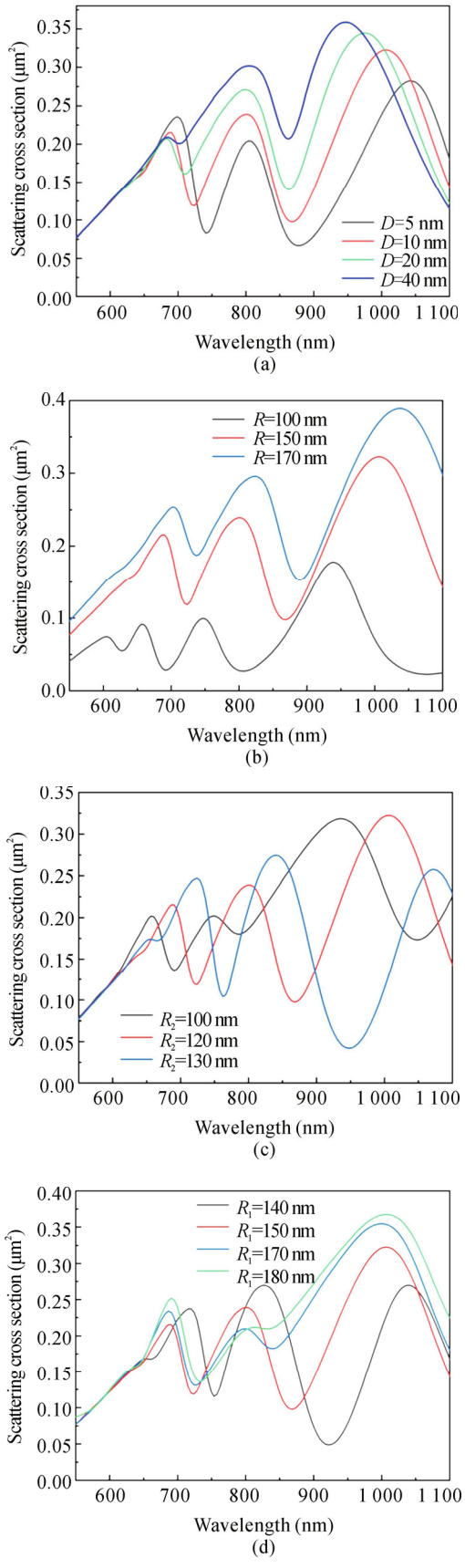

Fig.5 Dependence of scattering spectra of the disk-NCNR with ΔW=10 nm on the different values of (a) *D*, (b) *R*, (c) R_2 and (d) R_1 (Other parameters are the same as those used in Fig.2)

resonance becomes very weak, observed as a minor dip shown in Fig.5(a). The increase of *R* causes a red shift of the two dips, as shown in Fig.5(b), due to the red-shifted dipolar resonance of the disk with a larger size. What's particularly interesting is the occurrence of a new dip at 626 nm, which is attributed to the interaction of the hexadecapole of the NCNR with the dipole of the disk. It is thus implied that a relatively small disk is favor to the production of multiple Fano resonances, though the spectral intensity generated is somewhat weak due to less radiative damping of the bright mode. The two Fano resonances dependence on R_2 are obtained in Fig.5(c). With the increase of R_2, the enhanced coupling strength between the primitive modes gives rise to the NCNR modes with lower energies. This results in the two high-order multipolar modes closer to the dipole of the disk and accordingly two deeper dips. The effect of R_1 on the Fano resonances indicated in Fig.5(d) is strikingly different from others mentioned above. For the quadrupole-based Fano resonance, its dip is blue-shifted as R_1 increases and turns to be a minor valley when R_1 increases to 180 nm. While for the octupole one, it is blue-shifted first and then red-shifted a little, and the dip is unchanged much. It is well known that the resonance energy of the nanoring mode is determined by the primitive plasmon resonances and their interaction strength. When R_1 increases, the resonance wavelength of the primitive disk mode is red-shifted owing to phase retardation. On the other hand, due to the increased shell thickness, the reduction in coupling strength leads to blue-shifted hybridized resonances. As a result, there is a competition between the red shift for the increase of R_1 and the blue shift for the reduction in the coupling strength. For the quadrupole, the latter is the main contribution, while for the octupole, there is almost an equal effect when R_1=150 nm. Additionally, the variation in the two Fano dips could be ascribed to the mismatch in the resonance frequencies between the two higher-order modes and the dipole mode as R_1 increases. Thus, the Fano responses can be easily modified by tuning the geometric parameters.

Lastly, the sensing performance of the disk-NCNR structure as a biochemical sensor is evaluated by the *RI* sensitivity and *FOM*, respectively defined as the spectral shift of the Fano dip per *RI* unit (RIU) and the ratio of the *RI* sensitivity to the linewidth of the Fano resonance[29]. Fig.6(a) shows the scattering spectra of the disk-NCNR structure with Δ_x=20 nm embedded in different surrounding media with *RIs* from *n*=1 to *n*=1.3. As can be seen, the two Fano dips are significantly red-shifted with an increasing *RI* of the surrounding medium. When *RI* increases to *n*=1.3, the two dips shift to 897 nm and 1 102 nm, respectively. The corresponding *RI* sensitivities, calculated by a linear fit to the data obtained from the spectra, are up to 581 nm/RIU for octupolar Fano resonance and 780 nm/RIU for quadrupolar one, as shown in Fig.6(b). The Fano line widths acquired as the difference of the energies of the dip and peak are about 0.086 eV for octupolar Fano resonance and 0.103 eV for quadrupolar Fano resonance, and the corresponding *FOMs* reach as

large as 12.7 and 10.2, respectively. These sensing factors are better than those reported for the disk-disk structure[30], the nonconcentric ring-disk structure[29], and the nanoring dimer[31], and therefore the disk-NCNR would be a good platform for biosensing applications. It is noteworthy to point out that the *RI* sensitivity and *FOM* of the disk-NCNR structure calculated here are not optimal, and they could be further improved by better optimizing the geometric size.

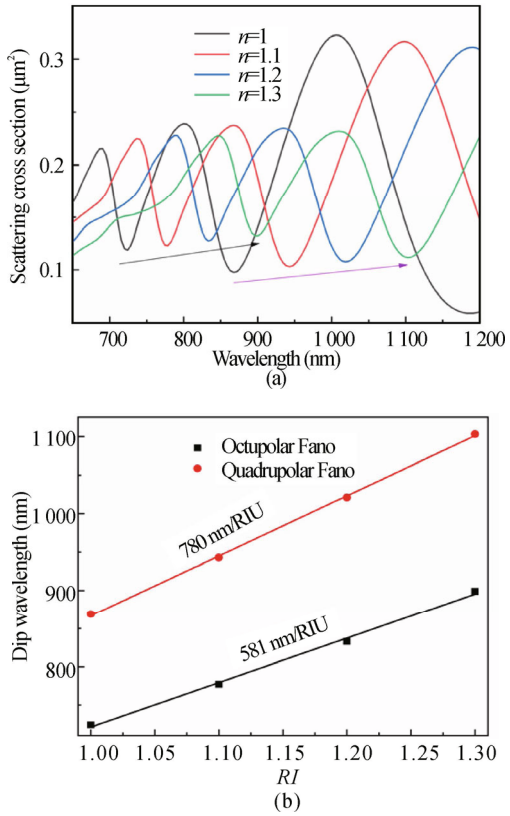

Fig.6 (a) Scattering spectra of the disk-NCNR with Δ_x=20 nm for different *RI*; (b) Dip wavelength shift versus *RI*

We have numerically investigated Fano properties of a plasmonic nanostructure consisting of a disk outside a nonconcentric ring based on the FDTD method. The calculated scattering spectra and electric field distributions show that two Fano resonances are induced due to the destructive interference of the dipole mode of the disk with the quadrupolar and octupolar modes of the ring. With increased symmetry breaking in the structure by offsetting the center of the inner surface of the ring, the two Fano resonances are red-shifted and experience different spectral changes. When the center of the inner surface gets closer to the disk, the Fano dips become less, while it moves far away from the disk, the octupole-based Fano dip grows and the quadrupolar Fano resonance changes not much. As the shell thickness is decreased by changing the inner or outer radius of the ring, the two Fano resonances are increased. The Fano resonances are also affected by the gap between the disk and the ring as well as the size of the disk. Furthermore, for the two Fano resonances, the *RI* sensitivities of 581 nm/RIU and 780 nm/RIU with *FOMs* of 12.7 and 10.2 can be respectively achieved. Such properties indicate that information about the target object can be extracted more accurately by processing the data obtained at different wavelengths simultaneously, making the structure useful for multi-wavelength sensing.

Ethics declarations

Conflicts of interest

The authors declare no conflict of interest.

References

[1] LIMONOV M, RYBIN M V, PODDUBNY A N, et al. Fano resonances in photonics[J]. Nature photonics, 2017, 11(9): 543-554.

[2] PILOZZI L, MISSORI M, CONTI C. Observation of terahertz transition from Fano resonances to bound states in the continuum[J]. Optics letters, 2023, 48(9): 2381-2384.

[3] LEE S C, BRUECK S. Analysis of Fano lineshape in extraordinary optical transmission[J]. Optics letters, 2022, 47(8): 2020-2023.

[4] LIMONOV M F. Fano resonance for applications[J]. Advances in optics and photonics, 2021, 13(3): 703-771.

[5] FENG G, CHEN Z, WANG Y, et al. Enhanced Fano resonance for high-sensitivity sensing based on bound states in the continuum[J]. Chinese optics letters, 2023, 21(3): 031202.

[6] DU M, SHEN Z. Enhanced and tunable double Fano resonances in plasmonic metasurfaces with nanoring dimers[J]. Journal of physics D: applied physics, 2021, 54(14): 145106.

[7] WU L, WANG Y, LIAO L, et al. Enhanced second-harmonic generation by Fano resonance of polaritons[J]. Applied physics express, 2021, 14(8): 082002.

[8] WANG J H, WANG S P, MELENTIEV P N, et al. SPASER as nanoprobe for biological applications: current state and opportunities[J]. Laser & photonics reviews, 2022, 16(7): 2100622.

[9] CHEN Z, ZHANG S, CHEN Y, et al. Double Fano resonances in hybrid disk/rod artificial plasmonic molecules based on dipole-quadrupole coupling[J]. Nanoscale, 2020, 12(17): 9776-9785.

[10] WANG Y, YU S, GAO Z, et al. Excitations of multiple Fano resonances based on permittivity-asymmetric dielectric meta-surfaces for nano-sensors[J]. IEEE photonics journal, 2022, 14(1): 1-7.

[11] RICCARDI M, MARTIN O J F. Role of electric currents in the Fano resonances of connected plasmonic structures[J]. Optics express, 2021, 29(8): 11635-11644.

[12] GHAHREMANI M, HABIL M K, ZAPATA-RODRIGUEZ C J. Anapole-assisted giant electric field enhancement for surface-enhanced coherent anti-Stokes Raman spectroscopy[J]. Scientific reports,

2021, 11(1): 10639.

[13] ZHAO H, FAN X, WEI X, et al. Highly sensitive multiple Fano resonances excitation on all-dielectric metastructure[J]. Optical review, 2023, 30(2): 208-216.

[14] HU H J, ZHANG F W, LI G Z, et al. Fano resonances with a high figure of merit in silver oligomer systems[J]. Photonics research, 2018, 6(3): 204-213.

[15] QI J, MIAO R, LI C, et al. Tunable multiple plasmon resonances and local field enhancement of a structure comprising a nanoring and a built-in nanocross[J]. Optics communications, 2018, 421: 19-24.

[16] ZHANG X, LIU F, YAN X, et al. Multipolar Fano resonances in concentric semi-disk ring cavities[J]. Optik, 2020, 200: 163416.

[17] ZHANG Y, HUO Y, CAI N, et al. Manipulation of multiple magnetic Fano resonances in nonconcentric asymmetric ring-ring nanostructure[J]. Materials research express, 2018, 5(2): 025012.

[18] WANG Z, REN L. High-order surface plasmonic resonance and near field enhancement in asymmetric nanoring/ellipsoid dimers[J]. Journal of applied spectroscopy, 2018, 85(3): 506-510.

[19] QIU R, LIN H, HUANG J, et al. Tunable multipolar Fano resonances and electric field enhancements in Au ring-disk plasmonic nanostructures[J]. Materials, 2018, 11(9): 1576.

[20] ZHANG Y, MING X, LIU G, et al. Narrow dark resonance modes in concentric ring/disk cavities[J]. Journal of the optical society of America B, 2015, 32(9): 1979-1985.

[21] LIU S, YUE P, ZHU M, et al. Restoring the silenced surface second-harmonic generation in split-ring resonators by magnetic and electric mode matching[J]. Optics express, 2019, 27(19): 26377-26391.

[22] HE J, FAN C, WANG J, et al. A giant localized field enhancement and high sensitivity in an asymmetric ring by exhibiting Fano resonance[J]. Journal of optics, 2013, 15(2): 025007.

[23] CUI J, JI B, SONG X, et al. Efficient modulation of multipolar Fano resonances in asymmetric ring-disk/split-ring-disk nanostructure[J]. Plasmonics, 2019, 14(1): 41-52.

[24] ZHANG X, YAN X, LIU F, et al. Symmetric and antisymmetric multipole mode-based Fano resonances in split theta-shaped nanocavities[J]. Plasmonics, 2021, 16(4): 1041-1048.

[25] TAFLOVE A, HAGNESS S. Computational electrodynamics: the finite-difference time-domain method[M]. Boston: Artech House, 2000: 19-45.

[26] JOHNSON P B, CHRISTY R W. Optical constants of the noble metals[J]. Physical review B, 1972, 6(12): 4370-4379.

[27] ZHANG X, LIU F, YAN X, et al. Symmetric and antisymmetric multipole electric-magnetic Fano resonances in elliptic disk-nonconcentric split ring plasmonic nanostructures[J]. Journal of optics, 2020, 22(11): 115003.

[28] ZHANG L, DONG Z, WANG Y M, et al. Dynamically configurable hybridization of plasmon modes in nanoring dimer arrays[J]. Nanoscale, 2015, 7(28): 12018-12022.

[29] HAO F, SONNEFRAUD Y, VAN DORPE P, et al. Symmetry breaking in plasmonic nanocavities: subradiant LSPR sensing and a tunable Fano resonance[J]. Nano letters, 2008, 8(11): 3983-3988.

[30] ZHANG Y, JIA T, ZHANG H, et al. Fano resonances in disk-ring plasmonic nanostructure: strong interaction between bright dipolar and dark multipolar mode[J]. Optics letters, 2012, 37(23): 4919-4921.

[31] DANA B D, KOYA A N, SONG X, et al. Effect of symmetry breaking on plasmonic coupling in nanoring dimers[J]. Plasmonics, 2020, 15(6): 1977-1988.